Surface-Initiated Nitroxide-Mediated Radical Polymerization of 4-Vinylpyridine on Magnetite Nanoparticles

Zhijun Chen,[1] Qingxiang Yang,[2] Kai Peng,[2] Yabing Guo[2]

[1]*Henan Provincial Key Laboratory of Surface and Interface Science, Zhengzhou University of Light Industry, Zhengzhou 450002*
[2]*Department of Polymer Science and Engineering, College of Materials and Chemical, Engineering, Zhengzhou University of Light Industry, Zhengzhou 450002*

Received 19 May 2009; accepted 6 July 2010
DOI 10.1002/app.33045
Published online 30 September 2010 in Wiley Online Library (wileyonlinelibrary.com).

ABSTRACT: Poly (4-vinylpyridine) (P4VP) brushes had been prepared by the surface-initiated nitroxide-mediated radical polymerization of 4-VP on the surface of 3-methacryloxyproyltrimethoxysilane (3-MPS)-modified magnetite nanoparticles with an average diameter of 30 nm. The grafting polymerization was accomplished by nitroxide-mediated polymerization of 4-VP, using 4-hydroxyl-2,2,6,6-tetramethyl-1-piperidinyl-oxy (HTEMPO·) free radical as capping agent and benzoyl peroxide (BPO) as initiator. X-ray photoelectron spectra (XPS) measurement demonstrated that the alkoxysilane initiator layer had formed on the magnetite surface. Gel permeation chromatograph analysis and XPS measurement suggested that the amount of grafted P4VP increases with increasing grafting time. The amount of P4VP grafted on the surface could be determined to be 0.09 chains/nm^2 by thermogravimetric analysis. The P4VP-grafted magnetite particles exhibited the characteristics of multidomain system, distinct from the single domain attributes of the pure magnetite particles. Atomic force-microscopy analysis revealed the diameter of the grafted P4VP magnetic latex particles is in the range of 120 nm to 150 nm. © 2010 Wiley Periodicals, Inc. J Appl Polym Sci 119: 3582–3590, 2011

Key words: magnetite; 3-methacryloxypropyltrimethoxysilane (3-MPS); 4-hydroxyl-2,2,6,6-tetramethyl-1-piperidinyloxy (HTEMPO·); poly(4-vinylpyridine) (P4VP); grafted; nitroxide mediated radical polymerization (NMRP)

INTRODUCTION

Recently, there have been increasing interests in tailoring the surface properties of magnetic nanoparticles by a polymer coating method for various functionalities. Such polymer-coated nanoparticles, due to their unique physical and chemical properties, have been used in the fields of biomedicine and bioengineering, such as enzyme immobilization,[1] cell separation,[2] protein purification,[3] and drug delivery.[4] Polymer-coated magnetic particles for a variety of applications can be prepared simply by altering the properties of the polymer shell, which is coated on nanoparticles through the connection of some stable and highly functional groups. Accordingly, it is vital to control the structures of the polymer shell, such as chain length and its distribution. Therefore, the development of efficient grafting strategies is becoming of greater and greater interest.

Grafting can be accomplished in a number of ways, including covalent attachment of functionalized polymers to reactive sites on an inorganic substrate surface (so-called "grafting to" technique),[5–7] or growth of polymer chains "from" initiators immobilized on solid substrate surface (so-called "grafting from" technique).[8–18] The grafting to method does not produce high density polymer layer due to the strong kinetic hindrance for the attachment of additional polymer chains to the surface. This kinetic hindrance impedes further film growth on the substrate surface.[7] In contrast, the grafting from strategies, as a promising approach pioneered by Sogah,[8] involves the immobilization of anchor molecules at the substrate surface. The initiating species will then be linked to these reactive units in one or more additional reaction steps. The major advantage of the grafting from way is the ability of yielding higher density polymer layer compared with those obtained from the conventional grafting to technique.

Atom transfer radical polymerization is an alternative approach to the synthesis of polymeric

Correspondence to: Z. Chen (mcchenzj@zzuli.edu.cn).
Contract grant sponsor: Natural Science Foundation of China; contract grant numbers: 20476101, 20976168.
Contract grant sponsor: Program for Science 65286 Technology Innovation Talents in Universities of Henan Province; contract grant number: 2008 HASTIT019.
Contract grant sponsor: Doctor Fund of Zhengzhou University of Light Industry.

brushes,[19,20] which uses the reversible activation of alkyl halides by transition metal catalysts to form radicals which propagate by the addition of monomer and provide "well defined" polymers.

In this study, we have applied a grafting from nitroxide mediated radical polymerization (NMRP) strategy to the graft polymerization of 4-vinylpyridine (4-VP) on alkoxysilane-functionalized magnetite (Fe_3O_4) nanopaticles in the presence of free radical initiator hydroxyl-2,2,6,6-tetramethyl-1-piperidinyloxy (HTEMPO·) catalyzed by BPO. We will discuss the attachment of 3-methacryloxypropyltrimethoxysilane (3-MPS) on the magnetite nanoparticles, the polymerization process of 4-VP, and the properties of the P4VP-grafted magnetic latex particles obtained in the following sections.

EXPERIMENTAL SECTION

The following chemicals were purchased: ferric chloride ($FeCl_3{\cdot}6H_2O$, 99%, Tianjin east China Factory of Reagents, China), ferrous sulfate ($FeSO_4{\cdot}7H_2O$, 99%, Tianjin Deen Chemical Reagents, China), sodium hydroxide (NaOH, 96%, Shandong Laiyang Chemistry and Chemical Engineering Factory, China), Methanol (CH_3OH, 99.5%, Suzhou Chemical Reagents Factory Anhui, China), Absolute ethanol (C_2H_5OH, 99.7%, Luoyang Haohua Chemical Reagents Factory, China), *n*-Hexane (C_6H_{14}, C. P. Guang Dong Yueqiao Chemical Factory, China), ($CH_2C(CH_3)COOC_3H_6$-$Si(OCH_3)_3$, 3-MPS, Nanjing Crompton Shuguang Organosilicon Specialties, China), benzoyl peroxide (BPO, 98%, Shanghai Jingxi Chemical Science and Technology, China). 4-VP (Aldrich, 95%) was dried by calcium hydride and then distilled under reduced pressure before use. BPO was recrystallized twice with methanol and then vacuum dried. HTEMPO· was prepared by oxidization of 4-hydroxyl-2,2,6,6-tetramethylpiperidine with 30% hydrogen peroxide, using sodium tungstate and ethylene diamine tetraacetic acid as catalyst.[21] All other reagents were used as received. Deionized water was used for all experiments.

Synthesis of magnetite nanoparticles

The magnetite nanoparticles were prepared by the conventional coprecipitation method.[22] Typically, 27 g of $FeCl_3{\cdot}6H_2O$ and 14 g of $FeSO_4{\cdot}7H_2O$ were dissolved in 250 mL deionized water under N_2 atmosphere. One hundred fifty milliliters of sodium hydroxide aqueous solution (2.7 mol L^{-1}) was then dripped into it while violently stirring for 15 min at 30°C. After aging for 3 h at 50°C the formed dark particles were washed with deionized water until neutrality. Finally, the obtained magnetite particles were collected by magnetic separation process and dried at 60°C under vacuum.

Magnetite nanoparticles coated by 3-MPS

The dried magnetite particles (8 g) were added into 400 mL of 95% ethanol aqueous solution (pH 4.78, adjusted with glacial acetic acid). The obtained solution was then treated by ultrasonication for 5 min. Subsequently, 8 mL 3-MPS ($CH_2C(CH_3)COOC_3H_6Si(OCH_3)_3$) was added and then the temperature was increased to 50°C under rapid stirring for 5 h. The resulted nanoparticles were washed with absolute ethanol for three times, and then dried at 60°C under vacuum.

Graft polymerization of 4-VP on the surface of 3-MPS modified magnetite

The graft polymerization was carried out according to Scheme 1. Typically, 50 mg treated magnetite, 28 mL 4-VP (0.1 mol), 48.4 mg BPO (0.2 mmol), and 62.0 mg HTEMPO· (0.36 mmol) were added into a three-necked flask with magnetic stirring; after degassing by three cycles of freeze-pump-thaw, the three-necked flask was placed into an oil bath at 95°C for 2 h and then at 130 ± 2°C under nitrogen atmosphere. For a desired time, the polymerization was stopped by cooling to 0°C. After polymerization, unreacted 4-VP monomer was removed by washing with methanol, and the P4VP-grafted magnetite particles were washed with methanol for several dispersion-magnetizing cycles to remove free P4VP produced from the free initiators. The free bulk P4VP polymerized was recovered by reprecipitation in toluene.

Characterization

Fourier transform infrared (FT-IR) spectra were obtained using a TENSOR 27 FTIR spectrometer by diffuse reflectance spectroscopy. X-ray photoelectron spectra (XPS) were recorded on an ESCA LB MK II electron spectrometer with nonmonochromatic Mg-$K\alpha$ radiation at 300W. Spectra are referenced to the C1s peak of carbon fixed at 285.0 eV. The BET (Brunauer, Emmett and Teller)-estimated surface area was determined by 3H-2000 Automatic surface area analyzer. Thermogravimetric analysis (TGA) was carried out using a Shimadzu DTG-60 with a standard sample of Al_2O_3. Samples were heated at 10 K/min under a nitrogen flow (15 mL/min). The molecular weight measurements were carried out by a Water 244 gel permeation chromatograph (GPC) with a UV detector using DMF as an eluent. Monodisperse polystyrene samples were used as standards for calibration. The average size and the morphology of samples were determined by a

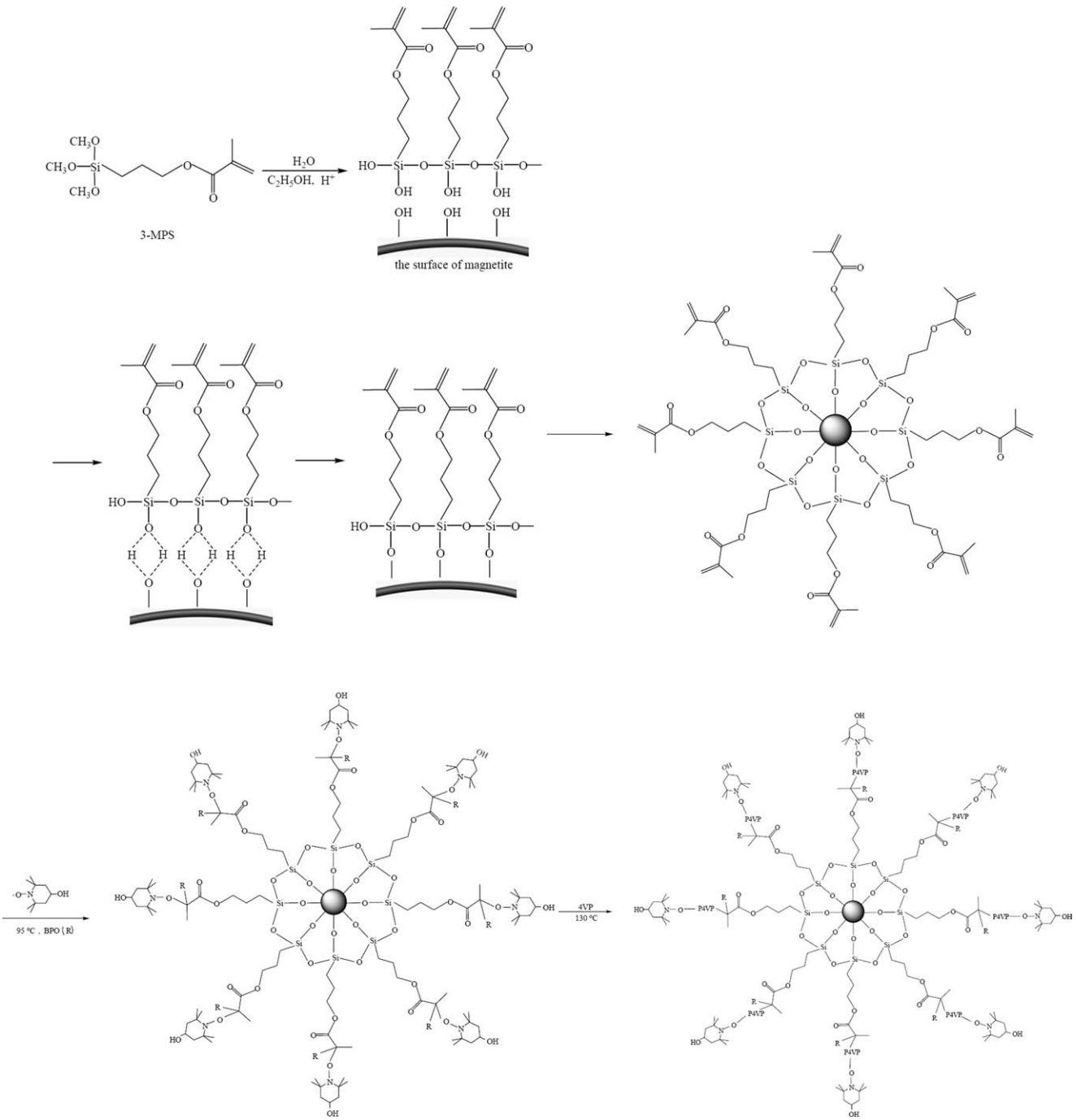

Scheme 1 Schematic representation for the grafting polymerization of 4-VP from treated magnetite.

Nanoscope MultiMode III atomic force microscope (AFM) from Digital Instruments in tapping mode. A rectangular cantilever with an integral sharpened silicon tip was used with a scan size of 1.0 μm and a rate of 1 Hz. Crystals of magnetite particles were examined by X-ray diffraction (XRD) using a Rigaku D/MAX23 A diffractometer operated at 35 kV and 20 mA, using Cu-Kα radiation (λ = 1.54 Å). The mean crystallite sizes of the powders of Fe_3O_4 were determined by the XRD–Scherrer formula (mean crystallite size = $0.9\lambda/(\beta \cos \theta)$, where β = broadening of width at half peak height in radians, and θ = Bragg angle.[23] The vibrating-sample magnetometer (VSM, LS7307-9309) was used to study the magnetic properties of magnetite particles at 300°C.

RESULTS AND DISCUSSION

Preparation of 3-MPS-coated magnetite nanoparticles

The organic layer on magnetite surface can be prepared by chemical coupling of silanes

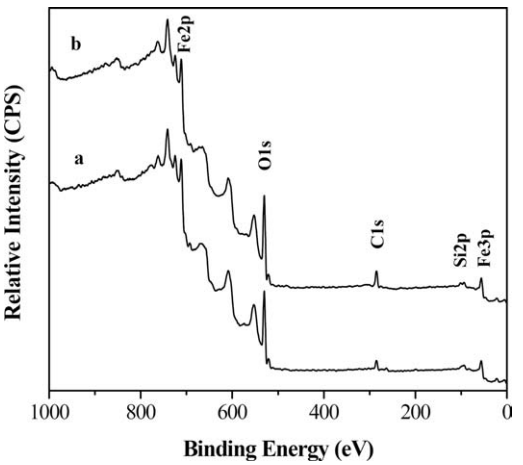

Figure 1 XPS wide scans spectra of (a) Fe_3O_4 substrate, (b) Fe_3O_4/3-MPS particles.

(e.g., N-(2-aminoethyl)-3-aminopropyltrimethoxysilane, AEAPS, and 3-aminopropyltriethoxysilane).[24,25] In our study, the alkoxysilane containing a vinyl group (—C=CH_2), 3-MPS, was coupled on the surface of the magnetite using an acidic aqueous silanization procedure. The silanization reaction is illustrated in Scheme 1. The 3-MPS is hydrolyzed in an acid aqueous solution that acts as a catalyst. Meanwhile, 3-MPS condenses with hydroxyl group of magnetite particles, and alkoxide groups (—OCH_3) are replaced by hydroxyl groups (—OH) to form reactive silanol groups, which condense with other silanol groups to produce siloxane bonds (Si—O—Si). The silane polymers were linked to the surface of the magnetite core by covalent bonding with the OH groups. Consequently, the silane polymers were attached onto the surface of magnetite core by covalent bonds. XPS spectra of the samples were used to examine whether the 3-MPS molecules had been anchored onto the surface of magnetic particle. Figure 1 showed the XPS wide scan spectra of those samples: (a) unmodified magnetite particles and (b) 3-MPS modified magnetite particles.

The wide scans are used primarily to provide an elemental composition of the surface and to determine whether any contaminants are present. For the Fe_3O_4 substrate surface, three major peaks are observed at 285 eV due to C 1s electrons, at 530 eV due to O 1s electrons, and at 711.5 eV due to Fe 2p electrons. A faint C 1s signal is observed in the spectrum of magnetite surface, even for the thoroughly cleaned magnetite nanoparticles substrate. The integrated area under C 1s peak and O 1s peak should provide the relative atomic concentration of carbon and oxygen in the magnetite particles substrate, with the ratio of relative intensity of C 1s to O 1s of $\sim$ 0.199. The observed carbon signal in the spectrum of magnetite surface is probably associated with the adsorption of CO_2 or the presence of a trace amount of carbonaceous contaminants on the surface of magnetite substrate. After 3-MPS silanization for 5 h, the ratio of relative intensity of C 1s to O 1s increased to 0.204. The survey scans are only suitable to determine elemental composition on the surface. To investigate the detailed changes in surface chemistry after silanization with 3-MPS for 5 h, narrow scans of the individual core level peaks are necessary. Narrow scan of C 1s spectrum is shown in Figure 2. The C 1s core-level photoemission peak is highly asymmetric, therefore, we are obliged to do curve fitting to explain the chemical structure of 3-MPS layer. According to the chemical structure of 3-MPS layer shown in Scheme 1, there should be four chemically distinct carbon environments in the 3-MPS layer. But in practice, XPS cannot distinguish CH_3 and CH_2 from C=C (bonding energy is 0.27 eV). Hence, we fitted the C 1s core-level photoemission peak with three peaks: the first peak at 284.67 eV, unambiguously assigned to carbons including the CH_2, CH_3, and C=C; the second carbon peak at 285.51 eV originates from the carbon bond to oxygen (CH_2—O); the third fitting peak at 290.56 eV bound to the carbon in ester linkage (O=C—O). These results show that the chemical structure of the silanized layer is consistent with the structure suggested in Scheme 1. Combining the analysis of XPS wide scans spectra in Figure 1, we can determine that the organosilane 3-MPS is covalently coupled to the surface of magnetite nanoparticles.

Surface-initiated NMRP of 4-VP on surface of the magnetite nanoparticles

Husseman et al.[26] reported that the polystyrene brushes on alkoxyamine surface could be prepared

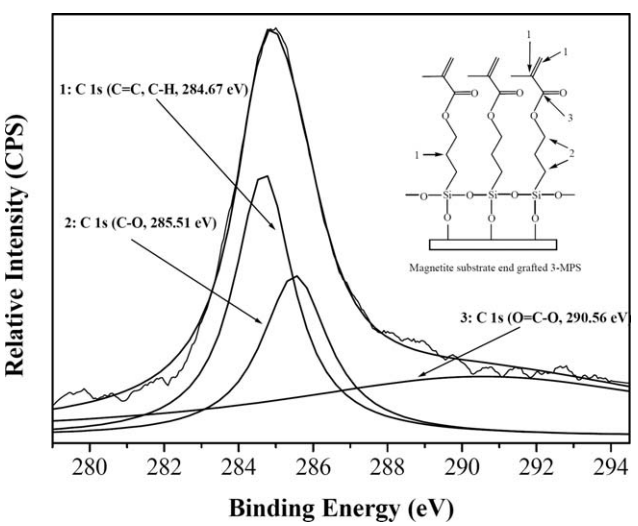

Figure 2 The narrow scans of the individual core level peaks C (1s) and fitting curves from Fe_3O_4/3-MPS particles (inset: structure of magnetite substrate end grafted 3-MPS).

TABLE I
Results of the Characterization of P4VP[a]

[HTEMPO·]/[BPO]	Reaction time (h)	$\overline{M}_n$	$\overline{M}_w/\overline{M}_n$
1.8	4	5815	1.17
	10	18,896	1.13
	24	40,096	1.20
	48	52,359	1.21
2.5	4	2186	1.13
	10	8421	1.15
	24	20,689	1.16
	48	32,149	1.17

[a] Obtained from bulk polymerization, [4-vinylpyridine], 0.26 mol, polymerization temperature, 130 ± 2°C.

from a 500 : 1 mixture of styrene and 1-phenyl-1-(2′,2′,6′,6′-tetramethyl-1′-piperidinyloxy) ethane. The polystyrene brushes have a number average molecular weight, $\overline{M}_n$, of 51,000 and a polydispersity of 1.14. These measurements are very close to the observed $\overline{M}_n$ and the polydispersity of the bulk free polystyrene, which are 48,000 and 1.20 respectively. To investigate the mechanism of the grafting polymerization, the grafting polymerization and bulk polymerization was repeated at 130°C with the same reaction prescription but varying the molar ratios of the HTEMPO· to BPO (4-VP/HTEMPO·/BPO= 1300/1.8/1, or 1300/2.5/1, molar ratio). We measured the molecular weight of bulk polymerization by a Waters 244 GPC with a UV detector using DMF as an eluent. Monodisperse polystyrene samples were used as standards for calibration. The number average molecular weight ($\overline{M}_n$) and polydispersities of polymerization of 4-VP of these reactions are listed in Table I. From Table I, we can find that the molecular weight of P4VP increases with increasing polymerization time, and the molecular weight distribution index is in the range of 1.13 to 1.21. These observations suggest that the polymerization in the presence of HTEMPO·/BPO initiator system is "living" free radical polymerization. With equal reaction time, when the concentration of HTEMPO· is lower, the molecular weight of resulting polymers is higher, and the distribution is broader. It is because that the free radicals from the decomposition of the initiators should be captured by HTEMPO·, the lower the concentration of HTEMPO· the higher the amount of the free radicals is, and the ratio of the traditional free radical polymerization to controllable free radical polymerization is larger, thus the molecular weight of resulting polymers is higher, and the distribution is broader.[27,28]

To determine the polymer chains of P4VP had been grafted onto the surface of 3-MPS modified magnetic particles, FT-IR spectrum was measured. As Figure 3 shows, the bands around 2930 cm^{-1} originate from stretching vibration of C-H bond in alkyl-substituent of P4VP. A weak peak at 1710.5 cm^{-1} is assigned to stretching vibration of C=N bond in the pyridine ring group of P4VP, two sharp absorption peaks at 1598.8 cm^{-1} and 1414.3 cm^{-1} are associated with a weak peak at 1557.8 cm^{-1} due to aromatic quadrant C=C stretching in the pyridine ring of P4VP. Furthermore, the bands locked at 1250-1000 cm^{-1} correspond to stretching vibration of C-ON bond in P4VP polymer chains. Other absorptions include a sharp peak in 822.3 cm^{-1} due to the stretching vibration of Si—C bond, bands in 643.9, 568.1, and 447.3 cm^{-1} due to the characteristic absorption bands of the Fe—O bond of Fe_3O_4 substrate. In addition, there are some peaks in the spectra which may be derived from the impurities, including the peak at 2367.1 cm^{-1} derived from environmental CO_2 molecules, and around 3443 cm^{-1} derived from absorption H_2O.

XPS measurements further confirmed that the P4VP were grafted onto the surface of alkoxysilane-functionalized magnetic particles. Figure 4 is the XPS wide scan spectra of P4VP-grafted magnetite particles with polymerization time of 24 h and 48 h. The Data on the surface chemical composition of the samples are given in Table II. As shown in Figure 4(a), after 24 h of grafting polymerization of 4-VP, one stronger peak than in Figure 1(b) at 285 eV due to C 1s electrons and another weaker peak than in Figure 1(b) at 530.5 eV originating from O 1s electrons were observed. The ratio of C 1s to O 1s relative intensity is $\sim$ 0.707, estimated from the integrated area of core-level photoemission peaks for these atoms in narrow scan spectra. This is much greater than the ratio of 0.204 in 3-MPS modified magnetite particles. Furthermore, a characteristic

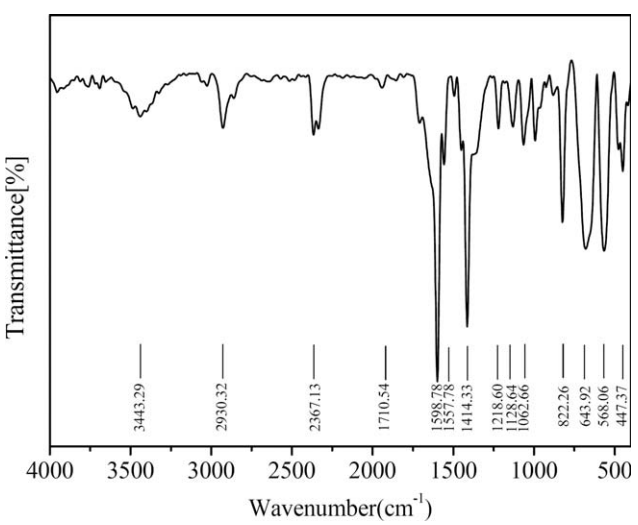

Figure 3 FT-IR spectrum of P4VP-grafted magnetite ([HTEMPO·]/[BPO] = 1.8, polymerization time, 48 h).

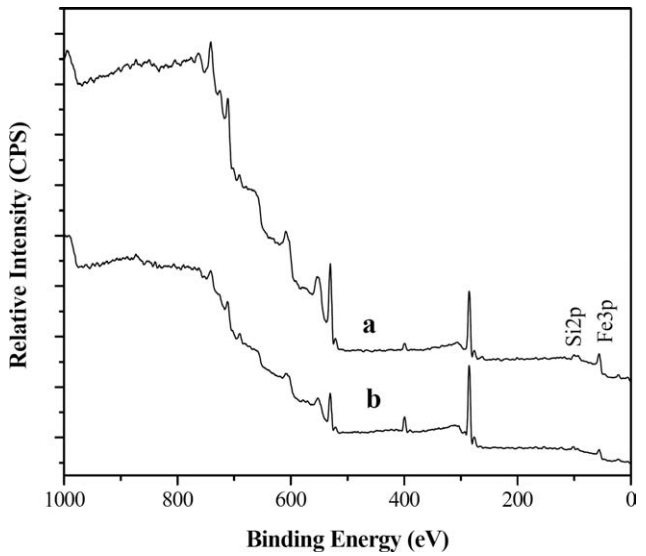

Figure 4 Wide scan spectra of P4VP-grafted magnetite particles at grafting polymerization time of 24 h (a) and 48 h (b). ([HTEMPO·]/[BPO] = 1.8) To entirely remove the ungrafted P4VP from the magnetite substrate surface, the samples were washed with excess methanol and separated by magnetic separation process.

peak of N 1s obviously observed at about 400 eV. These earlier observations suggest that the P4VP was chemically attached onto previous modified magnetite particles. In addition, for the sample with polymerization time of 48 h, as shown in Figure 4(b), the ratio of relative intensity of C 1s to O 1s increased to 2.054 and peak intensity of C 1s became dominant. On the other hand, from Table II, it is obvious that the atomic concentration of nitrogen increases with increasing grafting time, from 4.03 to 8.89%. It suggests that the amount of grafted polymer increases with increasing grafting time. So, it is possible to control the length of the polymer grafted on the magnetite particles by the control of grafting time.

To determine the specific surface area of the magnetic particles, a nitrogen adsorption method was employed and the BET equation was applied. The BET method is a universal approach used to determine the specific surface area of adsorbents and to characterize porous materials. The surface area of

TABLE II
Surface Chemical Composition of Grafted P4VP with HTEMPO· Chain End at Different Grafted-Polymerization Time ([HTEMPO·]/[BPO] = 1.8)

Time (h)	C%	N%	O%	Fe%	Si%
24	55.46	4.03	29.69	9.51	1.32
48	72.72	8.89	13.42	3.51	1.45

TABLE III
Weight Loss of Synthesized Sample

Sample[a]	Δm ($\times 10^{-2}$ mg)
1	7.9
2	38.2

[a] Sample 1, magnetite modified by 3-MPS; Sample 2, P4VP-grafted magnetite with grafting for 48 h and [HTEMPO·]/[BPO] = 1.8.

untreated magnetite particles was determined to be $\sim 38.88\ m^2/g$.

To estimate the amount of P4VP grafted on magnetite particles, TGA was conducted. Table III shows the weight loss of 3-MPS modified magnetite particles and P4VP grafted magnetite particles. The grafting density ($\sum$, chains/nm^2) of P4VP on magnetite particle was determined to be ~ 0.09 chains/nm^2, using the following equation on the basis of the BET-estimated surface area (σ, 38.88 m^2/g):

$$\sum(\text{chains/nm}^2) = \frac{(\Delta m_2 - \Delta m_1) \times N_A}{\sigma \times \overline{M}_n \times 10^{18}}$$

where $\triangle m_1$ and $\triangle m_2$, as shown in Table III, respectively, are the weight loss of 3-MPS modified magnetite particles and P4VP grafted magnetite particles from 100 to 600°C. These values correspond to the decomposition of the P4VP or silane in the surface of per 1 g untreated magnetite particles. N_A is Avogadro's number. The $\overline{M}_n$ represents the number average molecular weight of P4VP at bulk polymerization for 48 h with [HTEMPO·]/[BPO] of 1.8. The value of grafting density was relatively high compared to the "grafted-to" method.[23]

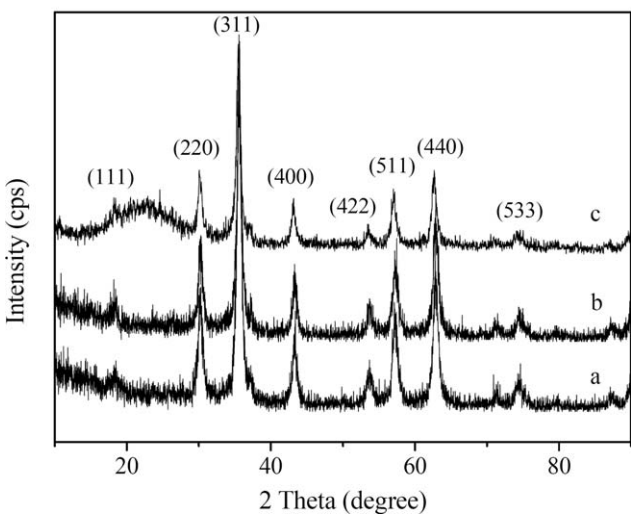

Figure 5 XRD patterns of (a) magnetite, (b) 3-MPS treated magnetite, and c P4VP-grafted magntite particles.

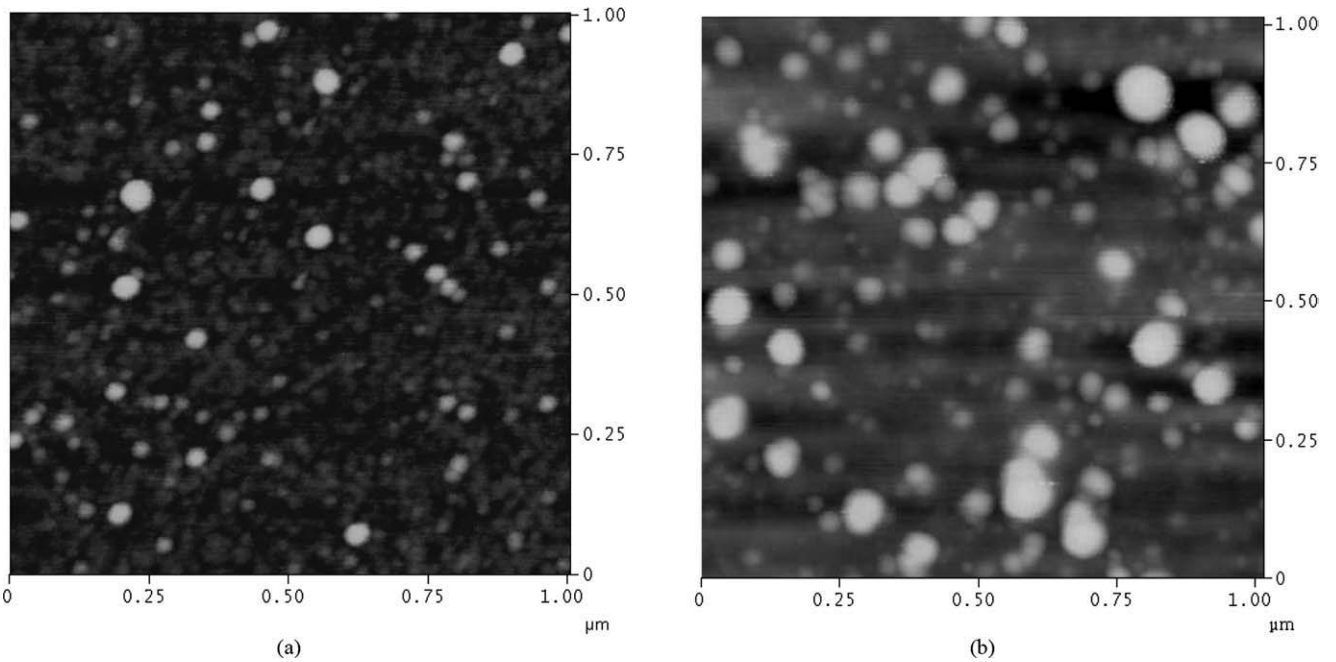

Figure 6 AFM height images of (a) magnetite and (b) P4VP-grafted magntite particles ([HTEMPO·]/[BPO] = 1.8, polymerization time, 48 h) attached to the Si surface at a scale. (X, Y range = 1000 nm) and different Z ranges (a = 20 nm, b = 150 nm)

Determination of the crystal structure and morphology of magnetic particles

The crystal structure was investigated with XRD method. Figure 5(a-c) displays the XRD pattern of untreated magnetic particles, 3-MPS treated magnetic particles, and P4VP-grafted magntite particles. The characteristic peaks [Fig. 5(a)] at 2θ angles correspond very well to the standard card of magnetite (JCPDS: 19-0629), which reveals that the sample can be identified as Fe_3O_4 with the spinel structure. Furthermore, the strong and sharp peaks of the magnetite particles indicate their good crystalline state. Through the comparison of the patterns in Figure 5 with the standard magnetite, it can be concluded that magnetite nanoparticles coated by silane coupler and P4VP are also of spinel structure. This means that the surface coating of 3-MPS and the grafting of P4VP do not change the crystal structure of magnetite particles. Other crystalline phases that could be assigned to impurities were not detected, which suggests the prepared magnetic particle is pure. Meanwhile, the amorphous region between 15 and 30 nm corresponds to the amorphous P4VP. In addition, based on Scherrer's equation,[29] the average sizes of magnetite nanocrystals can be calculated by using the strongest reflection planes (311). They are estimated to be $\sim$ 15 nm.

The morphology of the sample was characterized by AFM. Figure 6 is AFM images of (a) untreated magnetite particles and (b) P4VP-grafted magnetite particles in ethanol prepared by dropping their dispersion after sonication onto a silicon wafer. From Figure 6(a), it can be seen that the untreated magnetite particles were rather polydisperse, near spherical, with diameters in the range 10 to 60 nm. There is a difference in the grain size measurements by the means of AFM and XRD. The reason is well known. The grain size measured by AFM is the distances

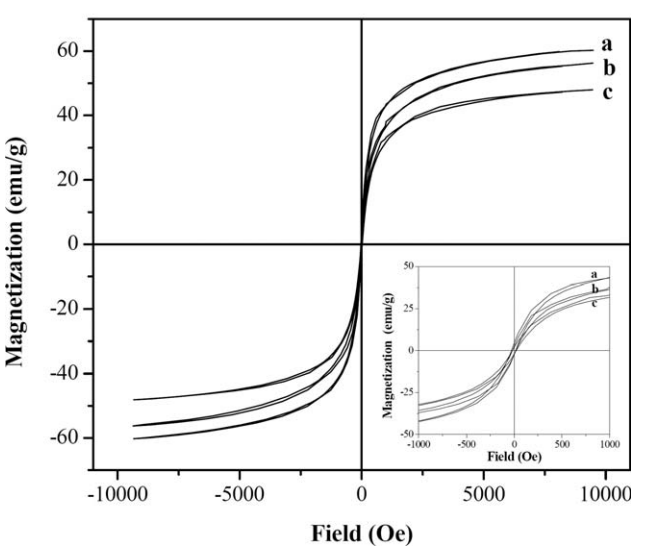

Figure 7 Hysteresis loop of (a) magnetite nanoparticles (sample a), (b) 3-MPS-magnetite nanoparticles (sample b) and (c) P4VP-grafted magntite composite particles (sample c, [HTEMPO·]/[BPO] = 1.8, polymerization time, 48 h) (the inset curse: hysteresis loop in the ranges from −1000 Oe to 1000 Oe).

TABLE IV
Magnetization Data for Various Samples Measured at Room Temperature

Sample	M_s (emu/g)	H_C (Oe)	M_r (emu/g)
a	60.3	22	3.4
b	56.3	18	2.3
c	48.2	19	1.9

between the visible grain boundaries. Whereas with XRD method, what is measured is the extent of the crystalline region that diffracts X-ray coherently. This is a more stringent criterion and therefore XRD method leads to smaller results. And interestingly, they tend to occur as dimmers. So their sizes increase to $\sim$ 120 and 150 nm.

Magnetic property

The magnetic properties of these magnetic particles were measured by room temperature VSM. Plotting of the magnetization with the applied magnetic field can render the hysteresis loop of the samples. Figure 7 is the hysteresis loop of the prepared samples: (a) untreated magnetite particles, (b) 3-MPS-treated magnetite nanoparticles, and (c) P4VP-grafted magnetite particles. In the case of Curve a, typical ferromagnetic behavior can be observed at low field range. And it can be asserted that the sample shown in Curve b is ferromagnetic as well. A weak ferromagnetic behavior was shown in Curve c. The saturation magnetization (Ms) are in the descending order: a $>$ b $>$c. The M_s of untreated magnetic particles is 60.3 emu/g, which is lower than that of the bulk phase (92 emu/g).[30] The reduction in M_s may be due to the larger ratio of nonmagnetic content to magnetic content of nanosized magnetite.[31] Consequently, the M_s of P4VP-grafted magnetite particles is the lowest among these samples since the surface of magnetite particles are wrapped with nonmagnetic polymer chains. The corresponding results from VSM, such as the values of remanent magnetization and coercive field for all samples are listed in Table IV. In Table IV, the coercive force changes in the following order: b $<$ c $<$ a. This trend can be well correlated to the sizes of the magnetic particles. The coercive force is known to follow a peak with the increase in crystallite size, and attains the maximum value at a critical size (D_c) it.[32] It is reported that the D_c of the magnetite nanocrystal is $\sim$ 20 and 29 nm.[33] Thus, P4VP-grafted magnetite particles (Sample c), having the largest particle size, fall in the right side of the peak, where the particles are of multidomain systems. In the case of 3-MPS-treated magnetite (Sample b) and pure magnetite (Sample a), as they had comparatively smaller crystallite sizes, their behavior could be related to that of a single domain system placed on the left side of the peak. Sample a possesses the maximum coercivity and Sample b has the lowest.

CONCLUSION

The following conclusions can be made on the basis of the experiments performed in this article. (1) Magnetite nanoparticles (particle size 10 to 60 nm) were synthesized by the coprecipitation of ferreous and ferrous solutions, and their surface was then chemically coupled by silane coupler to form grafting points of 4-VP. (2) The P4VP layer was prepared on the surface of the 3-MPS initiator layer by using a living-free-radical grafting polymerization in the presence of 4-hydroxy-2,2,6,6-tetramethylpiperidin-1-oxyl (HTEMPO·), and AFM reveals that P4VP-grafted magnetite particles have a size of 120 to 150 nm. (3) GPC analysis and XPS measurements suggests that the amount of grafted P4VP increases with increasing grafting time, which shows it is possible to control the length of the polymer grafted on the magnetite particles through the methods of living free radical polymerization. (4) From TGA measurement, the grafting density ($\sum$, chains/nm^2) of P4VP on magnetite particles was determined to be about 0.09 chains/nm^2 on the basis of the BET-estimated surface area (σ, 38.88 m^2/g). (5) VSM measurements demonstrates that the P4VP-grafted magnetite particles are weak ferromagnetic and the value of the saturation magnetization (48.2 emu/g) is significantly less than that of the untreated magnetite particles (60.3 emu/g), whereas, a multidomain system was attached to P4VP-grafted magnetite particles. This is different from the single domain system of pure magnetite nanoparticles. Because NMRP can be applied not only to homopolymerizations but also to block and/or random copolymerizations of a variety of monomers of styrene and its derivatives, this work will provide a new methodology to the synthesis of a wide range of high-performance polymer-coated magnetite particles.

References

1. Arica, M. Y.; Yavuz, H.; Patir, S.; Denizli, A. J Mol Catal B Enzym 2000, 11, 127.
2. Haik, Y.; Pai, V.; Chen, C. J. J Magn Magn Mater 1999, 194, 254.
3. Bucak, S.; Jones, D. A.; Laibinis, P. E.; Hatton, T. A. Biotechnol Prog 2003, 19, 477.
4. Lubbe, A. S.; Bergemann, C.; Brock, J.; McClure, D. G. J Magn Magn Mater 1999, 194, 149.
5. Lowe, A. B.; Sumerlin, B. S.; Donovan, M. S.; McCormick, C. L. J Am Chem Soc 2002, 124, 11562.
6. Corbierre, M. K.; Cameron, N. S.; Sutton, M.; Mochrie, S. G.; Lurio, L. B.; Rühm, A.; Lennox, R. B. J Am Chem Soc 2001, 123, 10411.

7. Yang, X.; Shi, J.; Johnson, S.; Swanson, B. Langmuir 1998, 14, 1505.
8. Hertler, W. R.; Sogah, D. Y.; Boettcher, F. P. Macromolecules 1990, 23, 1264.
9. Ohno, K.; Morinaga, T.; Koh, K.; Tsujii, Y.; Fukuda, T. Macromolecules 2005, 38, 2137.
10. Chen, Z. J; Peng, K.; Mi, Y. L. J Appl Polym Sci 2007, 103, 3660.
11. Li, C.; Benicewicz, B. C. Macromolecules 2005, 38, 5929.
12. Ejaz, M.; Ohno, K.; Tsujii, Y.; Fukuda, T. Macromolecules 2000, 33, 2870.
13. Quirk, R. P.; Mathers, R. T.; Cregger, T.; Foster, M. D. Macromolecules 2002, 35, 9964.
14. Prucker, O.; Ruhe, J. Macromolecules 1998, 31, 592.
15. Zhou, Q.; Fan, X.; Xia, C.; Mays, J.; Advincula, R. C. Chem Mater 2001, 13, 2465.
16. Zhou, Q.; Wang, S.; Fan, X.; Advincula, R. C.; Mays, J. Langmuir 2002, 18, 3324.
17. Kim, J-. B.; Bruening, M. L.; Baker, G. L. J Am Chem Soc 2000, 122, 7616.
18. Watson, K. J.; Zhu, J.; Nguyen, S. T.; Mirkin, C. A. J Am Chem Soc 1999, 121, 462.
19. Guerrini, M. M.; Charleux, B.; Vairon, J-. P. Macromol Rapid Commun 2000, 21, 669.
20. Min, K. J Polym Sci A Polym Chem 2002, 40, 892.
21. Kurosaki, T.; Lee, K. W.; Okawara, M. J Polym Sci Polym Chem 1972, 10, 3295.
22. Denga, Y.; Wanga, L.; Yang, W.; Fu, S.; Elaïssari, A. J Magn Magn Mater 2003, 257, 69.
23. Ouada, H. B.; Hommel, H.; Legrand, A. P.; Balardb, H.; Papirer, E. J Colloid Interface Sci 1988, 122, 441.
24. Ma, M.; Zhang, Y.; Yu, W.; Shen, H-. Y.; Zhang, H-. Q.; Gu, N. Colloids Surf A 2003, 212, 219.
25. Liu, X. Q.; Ma, Z. Y.; Xing, J. M.; Liu, H. Z. J Magn Magn Mater 2004, 270, 1.
26. Husseman, M.; Malmstrom, E. E.; McNamara, M.; Mate, M.; Mecerreyes, D.; Benoit, D. G.; Hedrick, J. L.; Mansky, P.; Huang, E.; Russell, T. P.; Hawker, C. J. Macromolecules 1999, 32, 1424.
27. Fischer, H. Macromolecules 1997, 30, 5666.
28. Fischer, H. J Polym Sci A Polym Chem 1999, 37, 1885.
29. Zaitsev, V. S.; Filimonov, D. S.; Presnyakov, I. A.; Gambino, R. J.; Chu, B. J. Colloid Interface Sci 1999, 212, 49.
30. Zhao, G.; Feng, J-. J.; Zhang, Q-. L.; Li, S. P.; Chen, H. Y. Chem Mater 2005, 17, 3154.
31. Montagne, F.; Mondain-Monvalb, O.; Pichot, C.; Mozzanega, H.; Elassaria, A. J Magn Magn Mater 2002, 250, 302.
32. Leslie-Pelecky, D. L.; Rieke, R. D. Chem Mater 1996, 8, 1770.
33. Lin, C-. R.; Chu, Y-. M.; Wang, S-. C. Mater Lett 2006, 60, 447.